

Determination of change in the land use and land cover of the Samsun Bafra Delta Plain from 1990 to 2020 using GIS and Remote Sensing Techniques

İnci Demirağ Turan ^{a,*}, Orhan Dengiz ^b, Sena Pacci ^b, David Tavi Agbor ^c

^a Samsun University, Faculty of Human and Social Sciences, Department of Geography, Samsun, Türkiye

^b Ondokuz Mayıs University, Faculty of Agriculture, Department of Soil Science and Plant Nutrition, Samsun, Türkiye

^c Department of Agronomic and Applied Molecular Sciences, Faculty of Agriculture and Veterinary Medicine, University of Buea, Cameroon

Abstract

Land use and land cover changes can have detrimental effects on the ecology, if they are not properly aligned with the characteristics of the land. This study aims to evaluate the temporal changes in land use and land cover of Bafra Delta plain, situated in the east of Samsun province. The region is one of the most significant plains within the Black Sea area. Remote sensing technique was utilized in this research which made use of Landsat images from 1990, 2000, 2010, and 2020. Supervised classification was applied in ENVI 5.3v software to perform calculations, resulting in six main classes. Field work was applied to classify the unclassified classes. The resulting six land use-land cover classes were agriculture lands, forest, dune, marshy, water surface, and artificial areas. To determine land use efficiency, analogue data was digitised and transferred to a GIS database. The agricultural areas occupy the largest portion of the plain, followed by hazelnut and artificial areas. The changes over the last decade, notably the growth of artificial areas and water surfaces, and the reduction of arable lands, highlight significant variations in size across the areas. Furthermore, the study indicated that remote sensing and geographic information system techniques play a crucial role in identifying and monitoring land cover and land use trends on a large-scale to produce accurate and timely data. Poorly adapted land use changes can cause major ecological damage. The aim of this study is to identify the changes over time in land use and land cover of Bafra Delta plain, located to the east of Samsun city and one of the most significant plains in the Black Sea region, using remote sensing techniques. To this end, Landsat images from 1990, 2000, 2010 and 2020 are utilized. To perform the calculations, ENVI 5.3v software was employed, applying a supervised classification technique that resulted in forming six main classes. Fieldwork was conducted to classify the unclassified classes. The resulting land-use and land-cover classes were agricultural land, forest, dunes, marshland, water surface, and artificial areas. To evaluate land-use efficiency, analogue data were digitalised and imported into a GIS database. The plain's most extensive land-use areas consist of agricultural lands, followed by hazelnut and artificial areas. In the last decade, the rise in artificial and water surfaces and the decline in agricultural areas highlights significant changes in the region's size. This study also emphasises the crucial role of remote sensing and geographic information system techniques in generating fast and consistent data for monitoring large-scale land cover and land use trends.

Keywords: Land use-land cover, change analysis, Bafra Plain

© 2024 Federation of Eurasian Soil Science Societies. All rights reserved

Article Info

Received : 09.07.2023

Accepted : 03.12.2023

Available online : xx.12.2023

Author(s)

İ. Demirağ Turan *

O.Dengiz

S.Pacci

D.T.Agbor



* Corresponding author

Introduction

Life on Earth, human progress, as well as scientific findings that elaborate the interactions between ecosystems and humans are highly dependent on land, making land the most valuable human asset on Earth necessary for development (Pflugmacher et al., 2019). Despite the indispensability of land to humans, land is undergoing a series of changes due to natural or anthropogenic activities called land use/land cover change (Liu et al., 2014). These changes have recently experienced massive investment in the form of research to provide checks and balances in global ecological fields (Samie et al., 2017). This can be seen in the publication of a catalogue of plans by the International Geosphere-Biosphere Programme (IGBP) and the International Human Dimensions Programme on Global Environmental Change (IHDP) to stimulate research in the field of land use/land cover (Wu, 2019; Song et al., 2020). Land use/land cover remains a topic of serious concern in recent times as it greatly affects global human progress as a critical component of climate change that alters ecosystem functions and services (Roy et al., 2022; Xu and Xiao, 2022). Hence, to furnish scientific evidence for natural resource management and global development, it is imperative to conduct investigations and assessments on the factors that drive land use and land cover changes. This is crucial for proper utilisation, allocation, and planning of land resources. (Cui et al., 2022). In this regard, remote sensing and GIS are critical tools for the study and analysis of land use/land cover (Hussain et al., 2020; MohanRajan, et al., 2020).

Remote sensing and GIS are effective methods for studying changes in land use and land cover, thanks to their ability to efficiently and technically cover a wide range of observations and provide a large amount of information over a small period. They are also valuable tools for monitoring the environmental impact of global human development. (Bansod and Dandekar, 2018; Nguyen et al., 2020). Remote sensing and GIS have the potential to deliver timely, precise, and dependable insights on changes in land use and land coverage over specific time intervals in a cost-effective and efficient way. (Chen et al., 2017; Govender et al., 2022). The study of land use/land cover change has brought remote sensing and GIS tools into focus for researchers. It is apparent that the IGBP and the United States Geological Survey (USGS) collaborated to create a global LULC data product with 1 km resolution, utilizing Advanced Very High Resolution Radiometer (AVHRR) data (Loveland et al., 2000). LULC change in the Yellow River Basin of Shandong Province was studied by Cui et al. (2022) using remote sensing and GIS from 2000 to 2020. Similar work was done by Stefanski et al. (2014), where they studied LULC change in western Ukraine from 1986 to 2010 using Landsat and ERS SAR data. The trend has been continued by other researchers such as Souza et al. (2020) in Brazil, Abdullah et al. (2019) in Bangladesh, and many others. In order to detect the changes associated with LULC attributes using the different satellite datasets, change detection involves using RS information to investigate the previous quantitative consequences of an event (Arora and Wolter 2018; Yasir et al., 2020). In order to perform supervised classifications, it is necessary to have prior knowledge of the scene areas, the area where a material of interest is located, the training sites, and the data to be retained and delimited for use in the algorithm (Orimoloye et al., 2018; Pushpanjali et al., 2022).

Climate change is an undeniable reality, with adverse effects on every country worldwide, including Turkey, and posing a significant threat to the livelihoods of small landowners and farmers. This is primarily because small-scale farmers heavily rely on agriculture for their survival, and the agricultural sector is the most vulnerable to climate change's impacts in contemporary times. Bafra is a district in Turkey's Samsun province, known for its rich soils and high quality tobacco growing conditions, making Bafra prominent in tobacco production. However, tobacco production in Bafra has recently declined drastically due to the adverse effects of climate change on the district, resulting in significant LULC changes in the area. Despite the evidence of land degradation in Bafra district, there has been no previous study of LULC changes over time, despite Bafra district's vulnerability status to climate change. Bafra district is facing hazardous situations due to traffic congestion, urbanisation leading to congestion, accidents and pollution as a result of the ever increasing population which is not keeping pace with the available resources. Therefore, there is a need for LULC change studies over a long period of time using GIS and remote sensing in Bafra district to provide information on the dynamics of LULC. Therefore, this paper investigates LULC change over a long time period of 30 years using GIS and remote sensing to identify different LULC change drivers, perform NDVI analysis, generate maps and detect change using satellite data.

Material and Methods

The study area description

This research was done in Samsun-Bafra delta plain district. The Bafra Plain is located in the central Black Sea region of Turkey (Figure 1). The research area is located 30 km to the west of the province of Samsun (4620-4600 km N- 230-260 km E UTM).



Figure 1. Location of the study area.

The area has a surface area of 72052 ha and lies at an elevation of 0-204 m above sea level with a semi-humid climate (Figure 2). Most of the study area has a slope of less than 2 percent (Figure 2). The area has four seasons; summers, autumn, warmer and spring with an average temperature of 6.9 °C in summer and 22.2 °C in summer. The area has mean temperature, rainfall and evaporation per annum of are 13.6 °C, 764.3 mm and 726.7 mm respectively. Mesic soil temperature and ustic moisture regimes are present at the study site (Soil Survey Staff, 1999) dominated by alluvial lands; Vertisol, Inceptisol and Entisol. The range of organic matter in soils is 1.70% to 5.92%, while soil EC and pH values are varying at 7.28 to 8.01 and 0.61-2.79 dSm⁻¹, respectively. The study area is mostly dominated by agriculture as economic activity with crops like maize, rice, maize, watermelon, pepper, cucumber, tomato and tobacco.

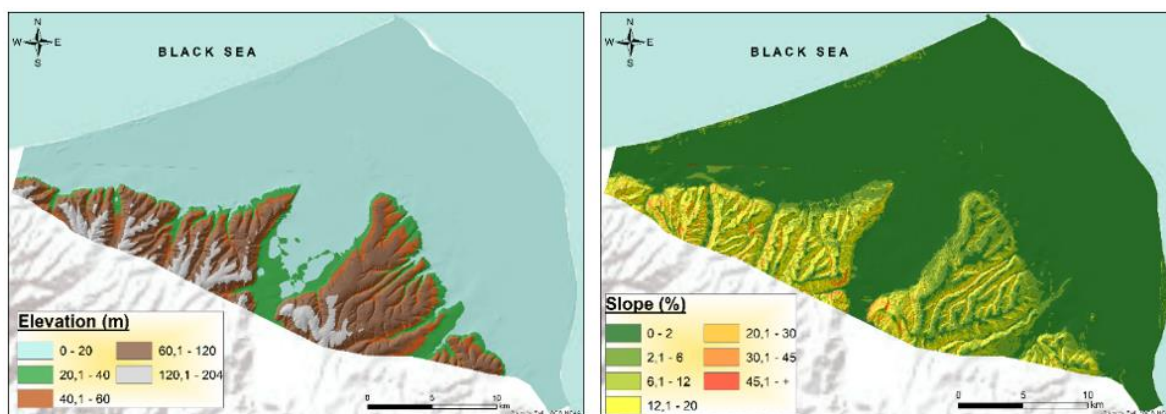


Figure 2. Elevation and slope map of the study area

Data collection

Land use and land cover changes, as well as alterations in NDVI and NDBI, were identified by using satellite images from Landsat 8, Thematic Mapper (TM) and Enhanced TM Plus (ETM+). For this study, Landsat satellite images were obtained for the years 1990, 2000, 2010 and 2020 (Figure 3). The images were downloaded easily and at no cost from the United States Geological Survey (USGS) through the earth explorer website (USGS, 2020), as displayed in Table 1.

Table 1. Landsat satellite image specifications

Data type	Date of Production	Sensor	Path/Row
Landsat image	25.05.1990	LANDSAT 5 /TM	175/31
Landsat image	20.05.2000	LANDSAT 5 /TM	175/31
Landsat image	30.04.2010	LANDSAT 5 /TM	175/31
Landsat image	26.05.2020	LANDSAT 8/ OLI_TIRS	175/31

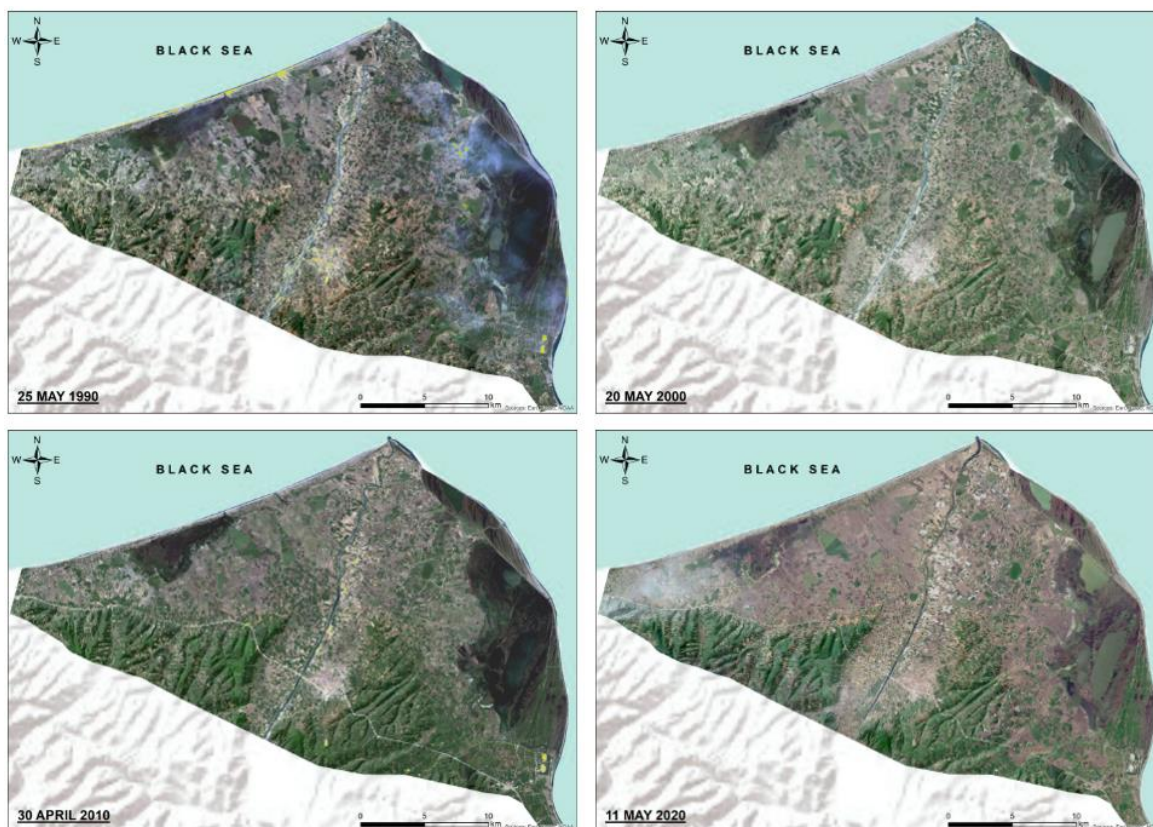


Figure 3. Satellite images for each year

Image classification

The Landsat images were created by combining bands 4, 3 and 1, achieved through layer stacking. Subsequently, using the extraction by mask tools and an image based on the study area, the subsetting procedure was executed in Arc GIS 10.1 software (Iqbal and Khan, 2014). The supervised classification method was used to classify the digital LULC data using field knowledge for the captured images. Supervised classification was utilised to produce LULC maps, while taking into consideration the study area. These LULC images were reclassified utilizing ArcGIS 10.7.1 which enabled us to compare the changes detected over time. The classification approach is graphically demonstrated in Figure 4. The LULC categories comprised farming, human-made (encompassing all facilities, business and housing units, roads and communities), sandbank zones (areas covered in sand), woodland areas, marshlands and bodies of water (rivers, lakes, ponds, canals, low-lying regions and marshes) (Aboelnour and Engel, 2018).

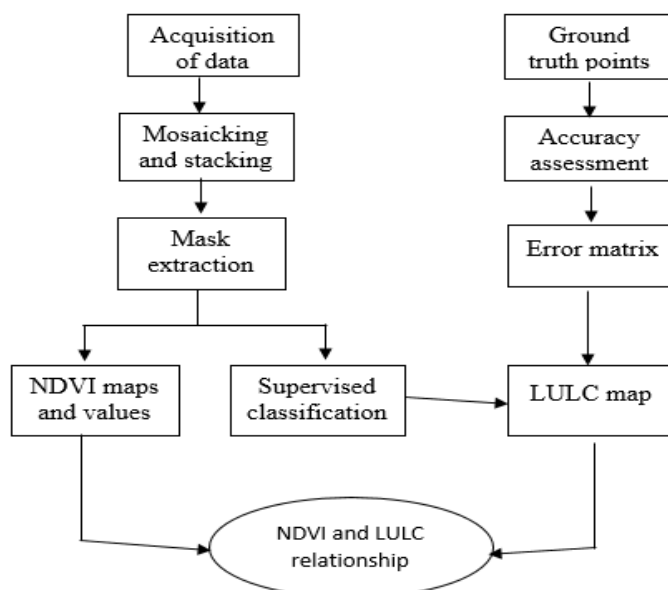


Figure 4. Classification approach

Accuracy assessment

A significant component in various processing procedures leading to image classification is accuracy (Lin et al., 2015; Ibharim et al., 2015). This gives the degree to which images classified are accurate to the natural reality termed error matrix (Lu et al., 2013). Accuracy gives the percentage to which the image classified using different statistical processes of image assessment is true (Zhang et al., 2016).

$$\text{Overall accuracy} = \frac{\text{number of sampled classes correctly classified}}{\text{number of reference sampled classes}} \quad (1)$$

The KHAT is the measure the magnitude to which RS classification falls in line with the reference data (Usman et al., 2015). KHAT is mathematical represented as follows:

$$K = \frac{\text{observed accuracy} - \text{chance assessment}}{1 - \text{chance agreement}} \quad (2)$$

Change of land use-land cover (LULC)

The current study aimed to evaluate multi-temporal land use/cover changes (LULC) by integrating GIS and remote sensing data. To this end, satellite imagery from Landsat 4 TM, Landsat 7 ETM, Landsat 5 TM, and Landsat 8 OLI-TIRS was used, spanning from May 1990 to May 2020 at an approximate 30 m resolution. The images were registered in Universal Transverse Mercator (UTM-m), zones 36N and WGS 84. The study included supervised classification and accuracy assessment stages. Six land use and land cover (LULC) classes were utilised: dune area, wetland, artificial area, agriculture area, water surface, and forest land. The maximum likelihood function of ENVI 5.1v was used for supervised classification. Furthermore, to validate the status of each LULC, ground control with GPS was conducted at specified coordinates during supervised classification.

Results and Discussion

Temporal change in land use and land cover

The present study utilised image processing to determine changes in land use/land cover from 1990 to 2020. Among all types of land, agricultural land had the highest coverage in the study area (Table 2). Figure 5 presents the land use/land cover distribution maps for different years. In 1990, agricultural land constituted 75.1% of the land use/land cover, but this has declined to 73.3% in 2020 (Table 2 and Figure 5). Forest land is present in regions where the gradient and elevation rise towards the south in the study area. In addition, the areas covered by water increased from 3.7% in 1990 to 5.0% in 2020. In this change, some places in the study area are changing as marsh areas and water areas. Artificial (all infrastructure, commercial and residential; road networks; and settlements distributed on the plain increased from about 3.8% in 1990 to 5.2% in 2000, and the distribution increased slightly in 2010 and reached 5.5%. In 2020, this rate has increased to 5.9%. This increase has been realized especially with the change from agricultural lands to artificial areas. With the increase of urbanization in different regions, land use land cover studies are increasing. Bağcı and Bahadır (2019) determined in their study that the proportion of water areas in the Kızılırmak Delta increased between 1987 and 2018, while agricultural areas from 359.1 km² to 347 km². In addition, similar results were obtained in the same study and they found that human activities increased from 45 km² to 63 km². Bağcı and Bahadır (2019) determined in their study that the proportion of water areas in the Kızılırmak Delta increased between 1987 and 2018, while agricultural areas from 359.1 km² to 347 km². In addition, similar results were obtained in the same study and it was determined that human activities increased from 45 km² to 63 km². Devkota et al. (2023) conducted their study in 12 rapidly urbanising cities of Nepal. Among these cities, Kathmandu city is experiencing a significant change. In this city, there is an increase of 65.61% in artificial areas between 2010 and 2020. In the same city, there is a decrease of -42.73% in agricultural areas.

Table 2. The changes in the area and proportional distributions of the land use land cover in the Bafra Plain for the years 1990, 2000, 2010 and 2020

LU/LC	1990		2000		2010		2020	
	ha	%	ha	%	ha	%	ha	%
Artificial area	2764	3.8	3719	5.2	3939	5.5	4276	5.9
Water bodies	2691	3.7	2895	4.0	3265	4.5	3596	5.0
Dune area	1572	2.2	1526	2.1	1502	2.1	1504	2.1
Marshy land	8859	12.3	8020	11.1	7960	11.0	7810	10.8
Forest area	2053	2.8	2205	3.1	2134	3.0	2074	2.9
Agriculture area	54113	75.1	53687	74.5	53252	73.9	52792	73.3
Total	72052	100.0	72052	100.0	72052	100.0	72052	100.0

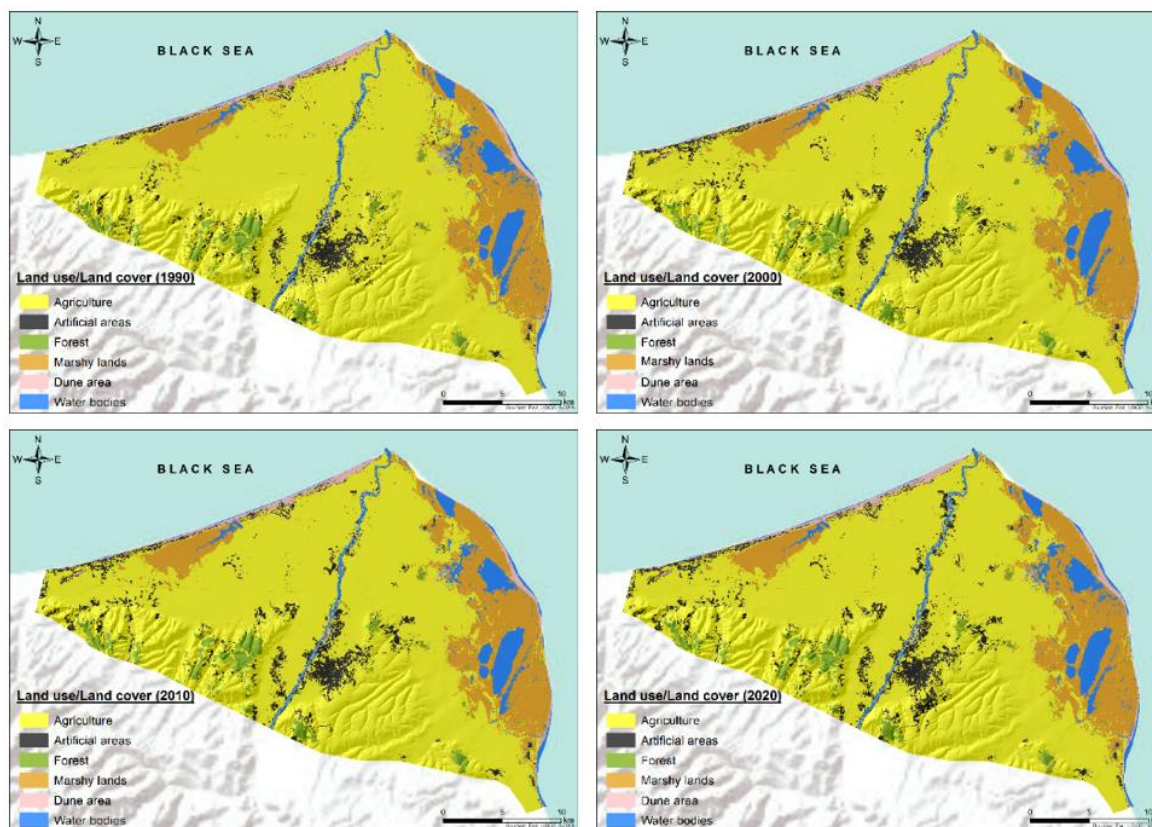


Figure 5. Land use/Land cover distribution maps for each year for the Bafra plain

Figure 6 depicts the percentage differences in total equivalent pixels within paired images classified during 1990 to 2020, with inter-period intervals of 1990-2000, 1990-2010, 2000-2010, 2000-2020, 2010-2020, and 1990-2020. These results obtained by the subtraction of total initial class count from total final count unveil the differences in land use and land coverage classes represented in the images. The most significant changes were observed between 1990 and 2020, followed by the changes from 1990 to 2010.

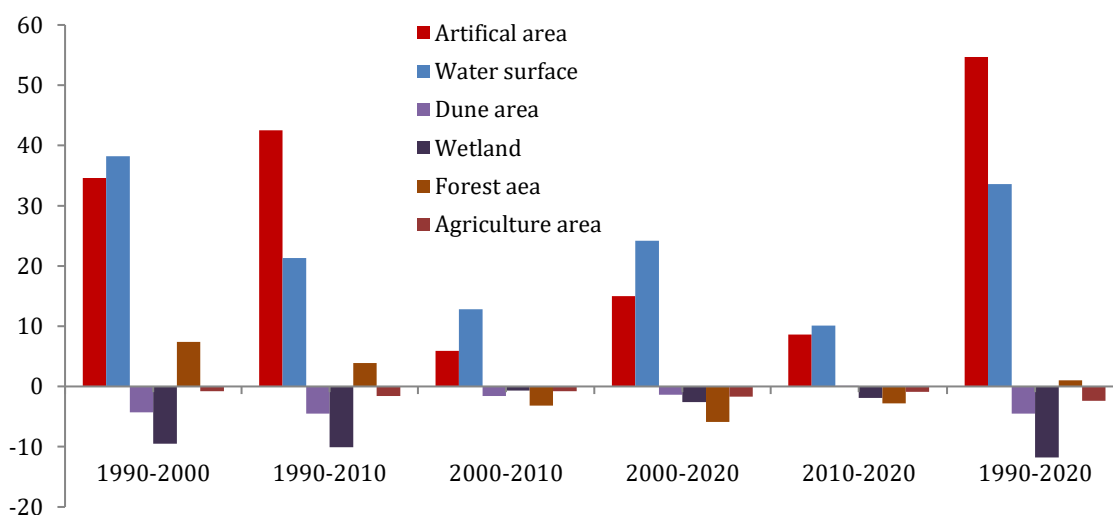


Figure 6. Land cover and land use differences for six time periods of the study area

The accuracy analysis results

Landsat (TM) satellite imagery of the study site taken on 20th May 1990, 20th May 2000, and 30th April 2010, as well as a Landsat-8 OLI satellite image captured on 26th May 2020, were analysed against 300 ground control points established during field investigations. The accuracy analysis results obtained after classification of each satellite image were given in Table 3. According to the results obtained, 90.66% accuracy was reached in the satellite image dated 20.05.1990. According to this value, the classification is considered to be accurate and reliable (Koç and Yener, 2001; Özdemir and Özkan, 2003). In addition, the kappa value of 0.88 indicates that the agreement between the observers is complete. The highest user accuracy in the image

was obtained from dune areas with 100 % (Table 3). In the satellite image dated 20.05.2000, 86.12 % accuracy was achieved for the classification results and it was determined that the agreement between the observers was complete with a kappa value of 0.84. The highest user accuracy was obtained from dune areas with 94.07%. The overall classification accuracy was 92.66% for artificial areas (92.66%), followed by marsh areas (91.20%), forest (82.15%), water areas (80.19%) and agricultural areas (80.02%). In the satellite image dated 26.05.2020, 92.65% accuracy was achieved for the classification results and the kappa value was 0.90, indicating that the agreement between the observers was complete. The highest user accuracy in the image was obtained from marshy lands with 98.65%.

Table 3. Accuracy analysis results obtained after classification of each satellite image

20.05.1990 (%) Overall Accuracy = % 90.66 Kappa Value = 0.88								
Class	Agriculture	Forest	Marshy lands	Dune areas	Artificial areas	Water bodies	Producer Accuracy	User Accuracy
Agriculture	44	0	4	1	1	0	88.26	92.2
Forest	2	49	4	0	0	0	84.53	78.13
Marshy lands	1	1	40	0	0	0	98.59	98.24
Dune areas	1	0	0	45	1	0	97.03	100
Artificial areas	1	0	0	4	48	0	94.19	91.44
Water bodies	1	0	2	0	0	50	85.19	89.1
Total	50	50	50	50	50	50		
20.05.2000 (%) Overall Accuracy = % 86.12 Kappa Value = 0.84								
Agriculture	44	0	4	1	1	0	81.15	84.64
Forest	2	49	4	0	0	0	84.46	90.34
Marshy lands	1	1	40	0	0	0	93.27	88.16
Dune areas	1	0	0	45	1	0	94.07	84.34
Artificial areas	1	0	0	4	48	0	93.76	83.94
Water bodies	1	0	2	0	0	50	79.89	89.63
Total	50	50	50	50	50	50		
30.04.2010 (%) Overall Accuracy = % 86.13 Kappa Value = 0.83								
Agriculture	45	0	4	1	1	0	80.02	85.14
Forest	1	48	4	0	0	0	82.15	89.20
Marshy lands	1	1	40	0	1	0	91.20	87.06
Dune areas	1	1	0	46	1	0	95.12	85.15
Artificial areas	1	0	0	3	47	2	92.66	82.98
Water bodies	1	0	2	0	0	48	80.19	90.23
Total	50	50	50	50	50	50		
11.05.2020 (%) Overall Accuracy = % 92.65, Kappa Value = 0.90								
Agriculture	45	0	2	2	1	0	89.32	93.22
Forest	1	49	3	0	0	0	85.13	88.18
Marshy lands	1	1	44	0	1	0	98.65	99.12
Dune areas	1	0	0	46	1	0	97.23	99.18
Artificial areas	2	0	0	2	47	0	93.11	90.20
Water bodies	0	0	2	0	0	50	95.19	95.10
Total	50	50	50	50	50	50		

In this study, the spatial arrangement of vegetation cover was mapped using NDVI data from annual images. The results are displayed in Figure 7.

Table 4 presents the areas and proportions of vegetation density classes within the NDVI maps. For 1990 NDVI images, the majority of the study area fell under the very weak and weak density classes, accounting for 52.5% of the total area. These were trailed by intensive (24.7%) and moderate density classes (22.7%). The 2000 NDVI mapping showed almost the same outcome. Table 4 also provides information regarding positive and negative trends in land productivity dynamics (LPD) between 1990 and 2020. Conversely, there is a decrease in the area exhibiting high plant density, indicating a negative trend. The data shows an increase in the area with low plant density. However, a small portion of the study area reflects an increase in high plant density, indicating a positive trend.

Furthermore, Figure 8 illustrates discrepancies in vegetation cover density over six time periods, with the least fluctuations occurring in 1990-2000, 1990-2010, 2000-2010, 2000-2020, 2010-2020 and 1990-2020.

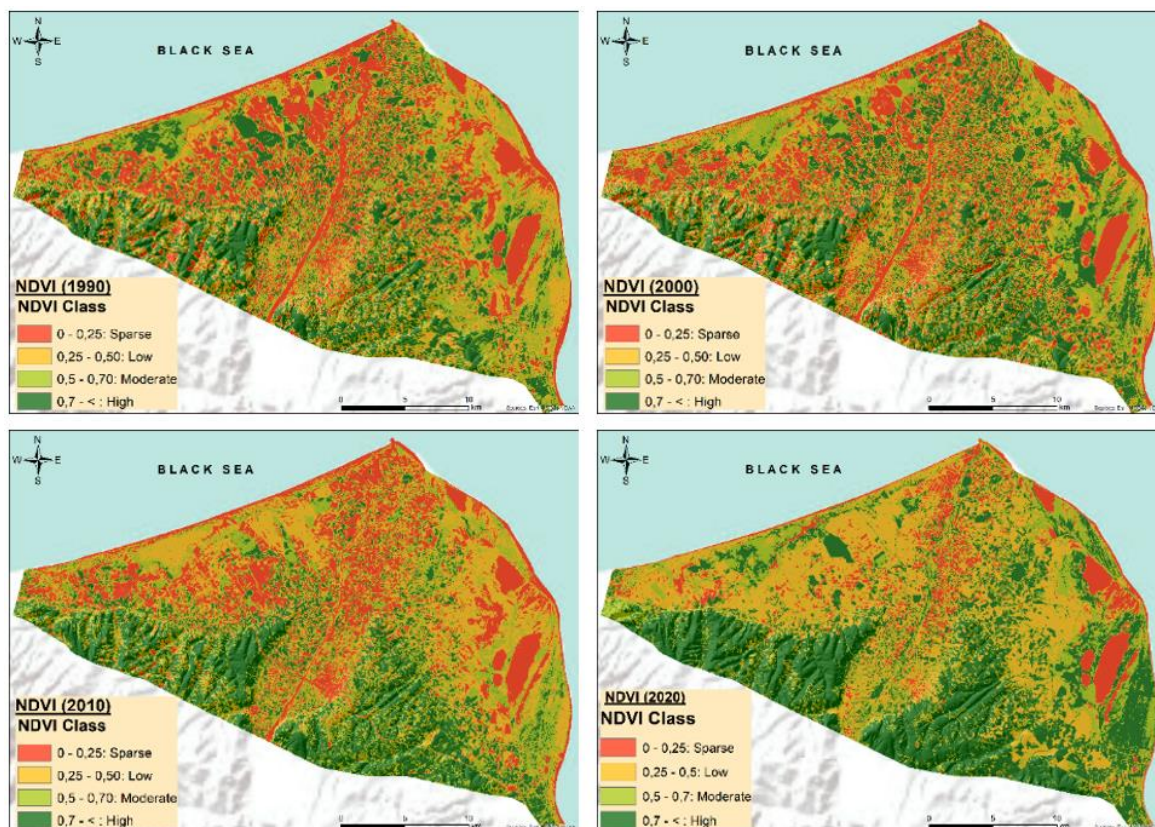


Figure 7. Maps of spatial distribution of plant density classes in 1990, 2000, 2010 and 2020 for the Bafra Delta Plain, Turkey

Table 4. Distribution of NDVI classes (area and %) for each year in the Bafra Delta Plain, Turkey

NDVI	1990		2000		2010		2020		Relative Change, % 1990-2020	Effect on LPD (-/+)
	ha	%	ha	%	ha	%	ha	%		
Very Weak 0-0.25	18548	25.74	16676	23.47	15991	22.19	7110	9.87	61.67	-
Weak 0.25-0.50	19289	26.77	17538	24.68	21714	30.14	24054	33.38	24.70	+
Moderate 0.50-0.70	16385	22.74	16898	23.78	16652	23.11	13867	19.25	22.23	-
Intensive > 70	17830	24.75	19940	28.06	17695	24.56	27021	37.50	51.55	+

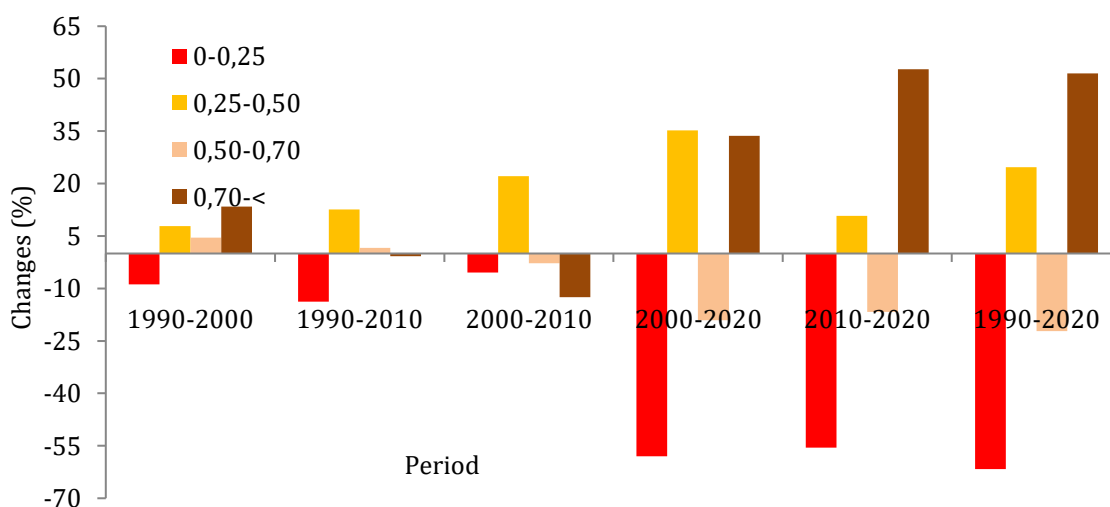


Figure 8. Vegetation density covers differences for six time periods Turkey

Conclusion

The review showcases the advancements of contemporary techniques for studying metalloids forms and heavy metals. In this present study, six different land use and land cover changes in the last thirty years (1990-2020) were analysed by using Landsat satellite images of Bafra Plain, the second largest plain of Turkey, from four different dates with 10-year intervals. An accuracy rate of more than 85% was obtained in the classification of satellite images. The areas with the highest distribution in the plain are arable agricultural lands, while the areas with the least distribution are dune areas. While agricultural lands were 75.1% in 1990, this rate decreased to 73.3% in 2020. In the study area, while artificial (all infrastructure, commercial and residential; road networks; and settlements) was around 3.8% in 1990, it increased to 5.2% in 2000, and the distribution increased slightly in 2010 and reached 5.5%. In 2020, this rate increased to 5.9 per cent.

The results of the study reveal that the pressure on agricultural lands in Samsun Bafra Plain has been increasing day by day in the last thirty years. It is thought that the findings of the study and the applied approach can be a source for periodically providing spatial data that can be used as the most important basis in the management activities of authorities and decision makers in order to determine time-dependent changes reliably and accurately in a short period of time. In the future, the study will be carried out with higher spatial, temporal and spectral resolutions.

References

- Abdullah, A.Y.M., Masrur, A., Adnan, M.S.G., Baky, M.A.A., Hassan, Q.K., Dewan, A., 2019. Spatio-temporal patterns of land use/land cover change in the heterogeneous coastal region of Bangladesh between 1990 and 2017. *Remote Sensing* 11(7): 790.
- Aboelnour, M., Engel, B.A., 2018. Application of remote sensing techniques and geographic information systems to analyze land surface temperature in response to land use/land cover change in Greater Cairo Region, Egypt. *Journal of Geographic Information System* 10(1): 57-88.
- Arora, G., Wolter, P.T., 2018. Tracking land cover change along the western edge of the US Corn Belt from 1984 through 2016 using satellite sensor data: Observed trends and contributing factors. *Journal of Land Use Science* 13(1-2): 59-80.
- Bağcı, H.R., Bahadır, M., 2019. Land use and temporal change in Kızılırmak Delta (Samsun) (1987-2019). *The Journal of Academic Social Science Studies* 78: 295-312. [in Turkish]
- Bansod, R.D., Dandekar, U.M., 2018. Evaluation of Morna river catchment with RS and GIS techniques. *Journal of Pharmacognosy and Phytochemistry* 7(1): 1945-1948.
- Chen, J., Theller, L., Gitau, M.W., Engel, B.A., Harbor, J.M., 2017. Urbanization impacts on surface runoff of the contiguous United States. *Journal of Environmental Management* 187: 470-481.
- Cui, J., Zhu, M., Liang, Y., Qin, G., Li, J., Liu, Y., 2022. Land use/land cover change and their driving factors in the Yellow River Basin of Shandong Province based on google earth Engine from 2000 to 2020. *ISPRS International Journal of Geo-Information* 11(3): 163.
- Devkota, P., Dhakal, S., Shrestha, S., Shrestha, U.B., 2023. Land use land cover changes in the major cities of Nepal from 1990 to 2020. *Environmental and Sustainability Indicators* 13: 100227.
- Govender, T., Dube, T., Shoko, C., 2022. Remote sensing of land use-land cover change and climate variability on hydrological processes in Sub-Saharan Africa: key scientific strides and challenges. *Geocarto International* 37(25): 10925-10949.
- Hussain, S., Mubeen, M., Ahmad, A., Akram, W., Hammad, H.M., Ali, M., Masood, N., Amin, A., Farid, H.U., Sultana, R.R., Fahad, S., Wang, D., Nasim, W., 2020. Using GIS tools to detect the land use/land cover changes during forty years in Lodhran District of Pakistan. *Environmental Science and Pollution Research* 27(32): 39676-39692.
- Ibharim, N.A., Mustapha, M. A., Lihan, T., Mazlan, A.G., 2015. Mapping mangrove changes in the Matang Mangrove Forest using multi temporal satellite imageries. *Ocean & Coastal Management* 114: 64-76.
- Iqbal, M.F., Khan, I.A., 2014. Spatiotemporal land use land cover change analysis and erosion risk mapping of Azad Jammu and Kashmir, Pakistan. *The Egyptian Journal of Remote Sensing and Space Science* 17(2): 209-229.
- Koç, A., Yener, H., 2001. Uzaktan algılama verileriyle İstanbul çevresi ormanlarının alansal ve yapısal değişikliklerinin saptanması. *İstanbul Üniversitesi, Orman Fakültesi Dergisi* 51(2): 17-36. [in Turkish]
- Lin, C., Wu, C.C., Tsogt, K., Ouyang, Y.C., Chang, C.I., 2015. Effects of atmospheric correction and pansharpening on LULC classification accuracy using WorldView-2 imagery. *Information Processing in Agriculture* 2(1): 25-36.
- Liu, J., Kuang, W., Zhang, Z., Xu, X., Qin, Y., Ning, J., Zhou, W., Zhang, S., Li, R., Yan, C., Wu, S., Shi, X., Jiang, N., Yu, D., Pan, X., Chi, W., 2014. Spatiotemporal characteristics, patterns, and causes of land-use changes in China since the late 1980s. *Journal of Geographical Sciences* 24(2): 195-210.
- Loveland, T.R., Reed, B.C., Brown, J.F., Ohlen, D.O., Zhu, Z., Yang, L.W., Merchant, J.W., 2000. Development of a global land cover characteristics database and IGBP DISCover from 1 km AVHRR data. *International Journal of Remote Sensing* 21(6-7): 1303-1330.
- Lu, D., Li, G., Moran, E., Hetrick, S., 2013. Spatiotemporal analysis of land use and land cover change in the Brazilian Amazon. *International Journal of Remote Sensing* 34(16): 5953-5978.

- MohanRajan, S.N., Loganathan, A., Manoharan, P., 2020. Survey on Land Use/Land Cover (LU/LC) change analysis in remote sensing and GIS environment: Techniques and Challenges. *Environmental Science and Pollution Research* 27(24): 29900-29926.
- Nguyen, L.H., Joshi, D.R., Clay, D.E., Henebry, G.M., 2020. Characterizing land cover/land use from multiple years of Landsat and MODIS time series: A novel approach using land surface phenology modeling and random forest classifier. *Remote Sensing of Environment* 238: 111017.
- Orimoloye, I.R., Mazinyo, S.P., Nel, W., Kalumba, A.M., 2018. Spatiotemporal monitoring of land surface temperature and estimated radiation using remote sensing: human health implications for East London, South Africa. *Environmental Earth Sciences* 77: 77.
- Pushpanjali, Osman, M.D., Srinivas, R.K., Kumar, P.P., Josily, S., Karthikeyan, K., Sammi, R.K., 2022. Land-use change mapping and analysis using remote sensing and GIS for watershed evaluation-A case study. *Journal of Soil and Water Conservation* 21(1): 1-6.
- Özdemir, İ., Özkan, Y.U., 2003. Monitoring the changes of forest areas using landsat satellite images in Armutlu forest district. *Süleyman Demirel Üniversitesi Orman Fakültesi Dergisi* 4(1): 55-66. [in Turkish]
- Pflugmacher, D., Rabe, A., Peters, M., Hostert, P., 2019. Mapping pan-European land cover using Landsat spectral-temporal metrics and the European LUCAS survey. *Remote Sensing of Environment* 221: 583-595.
- Roy, P.S., Ramachandran, R.M., Paul, O., Thakur, P.K., Ravan, S., Behera, M.D., Sarangi, C., Kanawade, V.P., 2022. Anthropogenic land use and land cover changes—A Review on its environmental consequences and climate change. *Journal of the Indian Society of Remote Sensing* 50: 1615–1640.
- Samie, A., Deng, X., Jia, S., Chen, D., 2017. Scenario-based simulation on dynamics of land-use-land-cover change in Punjab Province, Pakistan. *Sustainability* 9(8): 1285.
- Soil Survey Staff, 1999. Soil taxonomy: A basic of soil classification for making and interpreting soil survey. USDA Natural Resources Conservation Service, Agriculture Handbook No: 436. Washington DC, USA. Available at [Access date: 09.07.2023]: <https://www.nrcs.usda.gov/sites/default/files/2022-06/Soil%20Taxonomy.pdf>
- Stefanski, J., Chaskovskyy, O., Waske, B., 2014. Mapping and monitoring of land use changes in post-Soviet western Ukraine using remote sensing data. *Applied Geography* 55: 155-164.
- Song, W., Song, W., Gu, H., Li, F., 2020. Progress in the remote sensing monitoring of the ecological environment in mining areas. *International Journal of Environmental Research and Public Health* 17(6): 1846.
- Souza, C.M., Jr., Z. Shimbo, J., Rosa, M.R., Parente, L.L., A. Alencar, A., Rudorff, B.F.T., Hasenack, H., Matsumoto, M.G., Ferreira, L., Souza-Filho, P.W.M., de Oliveira, S.W., Rocha, W.F., Fonseca, A.W., Marques, C.B., Diniz, C.G., Costa, D., Monteiro, D., Rosa, E.R., Vélez-Martin, E., Weber, E.J., Lenti, F.E.B., Paternost, F.F., Pareyn, F.G.C., Siqueira, J.A., Viera, J.L., Neto, L.C.F., Saraiva, M.M., Sales, M.H., Salgado, M.P.G., Vasconcelos, R., Galano, S., Mesquita, V.V., Azevedo, T., 2020. Reconstructing three decades of land use and land cover changes in brazilian biomes with landsat archive and earth engine. *Remote Sensing* 12(17): 2735.
- USGS, 2020. USGS EarthExplorer. Available at [Access date: 15.05.2020]: <https://earthexplorer.usgs.gov/>
- Usman, M., Liedl, R., Shahid, M. A., Abbas, A., 2015. Land use/land cover classification and its change detection using multi-temporal MODIS NDVI data. *Journal of Geographical Sciences* 25(12): 1479–1506.
- Wu, J., 2019. Linking landscape, land system and design approaches to achieve sustainability. *Journal of Land Use Science* 14(2): 173-189.
- Xu, J., Xiao, P., 2022. A bibliometric analysis on the effects of land use change on ecosystem services: Current status, progress, and future directions. *Sustainability* 14(5): 3079.
- Yasir, M., Hui, S., Binghu, H., Rahman, S. U., 2020. Coastline extraction and land use change analysis using remote sensing (RS) and geographic information system (GIS) technology—A review of the literature. *Reviews on Environmental Health* 35(4): 453-460.
- Zhang, Z., Liu, S., Wei, J., Xu, J., Guo, W., Bao, W., Jiang, Z., 2016. Mass change of glaciers in Muztag Ata–Kongur Tagh, Eastern Pamir, China from 1971/76 to 2013/14 as derived from remote sensing data. *PLoS One* 11(1): e0147327.